

Numerical analysis of failure modeling in clinching process chain simulation

Christian R. Bielak^{1,a*}, Max Böhnke^{1,b}, Johannes Friedlein^{2,c}, Mathias Bobbert^{1,d}, Julia Mergheim^{2,e}, Paul Steinmann^{2,f} and Gerson Meschut^{1,g}

¹Laboratory for Material and Joining Technology (LWF), Paderborn University, Pohlweg 47-49, 33098 Paderborn, Germany

²Institute of Applied Mechanics, Friedrich-Alexander-Universität Erlangen-Nürnberg, Egerlandstrasse 5, 91058 Erlangen, Germany

^aChristian.Bielak@lwf.upb.de, ^bMax.Boehnke@lwf.upb.de, ^cJohannes.Friedlein@fau.de,

^dMathias.Bobbert@lwf.upb.de, ^eJulia.Mergheim@fau.de, ^fPaul.Steinmann@fau.de,

^gMeschut@lwf.upb.de

Keywords: Finite Element Method, Damage, Joining

Abstract. The application of the mechanical joining process clinching allows the assembly of different sheet metal materials with a wide range of material thickness configurations, which is of interest for lightweight multi-material structures. In order to be able to predict the clinched joint properties as a function of the individual manufacturing steps, current studies focus on numerical modeling of the entire clinching process chain. It is essential to be able to take into account the influence of the joining process-induced damage on the load-bearing capacity of the joint during the loading phase. This study presents a numerical damage accumulation in the clinching process based on an implemented Hosford-Coulomb failure model using a 3D clinching process model applied on the aluminum alloy EN AW-6014 in temper T4. A correspondence of the experimentally determined failure location with the element of the highest numerically determined damage accumulation is shown. Moreover, the experimentally determined failure behavior is predicted to be in agreement in the numerical loading simulation with transferred pre-damage from the process simulation.

Introduction

Clinching is a widely applied mechanical joining technique for sheet metal materials in which the joint is based on cold forming of the parts to be joined and no auxiliary element is required. It has proven particularly useful for the implementation of multi-material designs, which have become important in the context of lightweight construction in the automotive industry [1].

The material combination and clinching process parameters examined in this paper has been extensively investigated in [2]. In particular, the process chain of clinching aluminum EN AW-6014 T4 was described and experimental techniques were proposed to analyze the process-structure-property relationships from the sheet metals properties to the joined structure. 2D rotationally symmetric FE-models of this connection were presented in [3] and for 3D FE-models in [4]. With the FE models, results have already been obtained with regard to the joining point properties and the maximum transmissible force under load, which are in agreement with the experiments. The prediction of a neck crack in the joining process or the maximum strain under load could not be predicted yet due to a lack of damage and failure model in own previous studies. The plastic behavior and the pre-damage introduced into the material are relevant for the subsequent joining point properties. In [5] an isotropic elasto-plastic law coupled with a Lemaitre ductile damage model was used to investigate the clinching process. Subsequent strength tests and optimization of the process parameters through a Kriging metamodel were shown. In [6] the self-

piercing riveting process (SPR) was examined and it was shown that the consideration of the damage behavior during the joining process itself is of major importance. From this, they conclude that it might also be relevant to investigate damage evolution for clinching, which is a similar joining technique.

In [7] a damage model was developed in order to analyse process-induced defects during SPR and clinching. 6xxx series aluminium sheets in the T6 condition were investigated with limited ductility and different damage criteria were compared to predict the influence of process-induced damage on the strength properties of the joints.

Failure modeling in mechanical joining processes was presented in [8] by applying the GISSMO damage model in LS-DYNA to the SPR process simulation to predict ductile damage in thin aluminum sheets. The parameters for this stress state dependent material model have been identified from tensile tests with various characteristic stress states. In [9], the complete process chain for self-pierce riveting was numerically investigated with respect to joint failure. The calibration of damage models and their application in strength analysis are integral parts of the present study. Furthermore, different damage models and the influence of the setting depth on the joint strength and the type of joint failure are compared.

In [10] a method for the calibration of failure models for the simulation of clinching processes was presented. Based on experimental tests and corresponding simulation models, failure-relevant data were transferred into three different failure models and calibrated. The Hosford-Coulomb model [11] was found to be highly predictive.

The purpose of this study is to investigate the numerical damage accumulation in the clinching process based on an implemented Hosford-Coulomb failure model using a 3D clinching process model and the influence of the transferred damage on the load-bearing behavior under shear tensile load.

Finite-Element-Models

The FE-model used in this study for the calculation of the clinch joining process was first presented in [12] and then applied for a numerical process chain in [4]. The tool and sheet geometries as well as boundary conditions were adapted. All simulations run with the LS-DYNA Solver `ls-dyna_smp_d_R12.1` with implicit time integration. Due to the process time and low dynamic effects an implicit time integration was chosen.

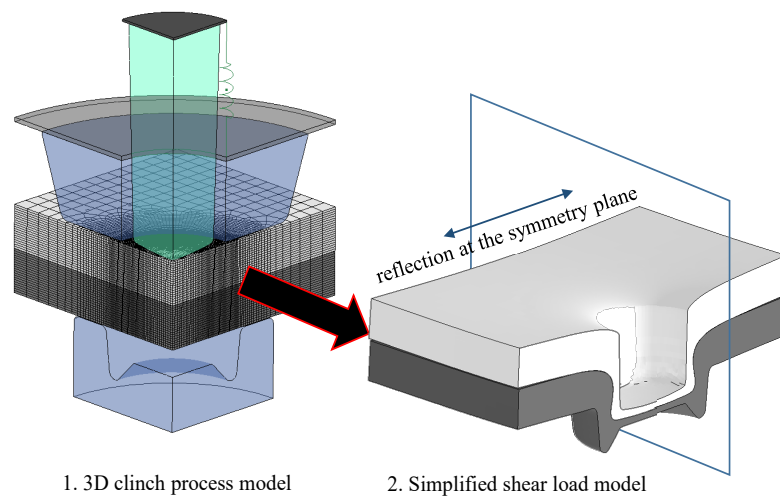


Fig. 1: FE clinch process and shear tensile test model

A clinch joining process model as well as a shear tensile model were used in this study. Pre-operation before joining, such as pre-strain, is not taken into account in this study. The models are

modified with respect to the element formulation of the sheet materials and the material model used. Since the discretization of the parts to be joined is optimized for the process, there is no need for automatic adaptive remeshing during the simulation. The sheets are now discretized with hexahedral elements, as shown in Fig. 1.

The clinching process takes advantage of the symmetry of the process and is calculated using a quarter model of the real geometry. The shear tensile test is based on the geometry calculated in the clinching process and the material conditions. This is represented by a reflection at the symmetry plane as half a model. The shear tensile test is simplified in terms of geometry and does not reproduce the real specimen stiffness from the experiment. This must be taken into account in the subsequent evaluation.

Material model

A hyperelastic-based finite plasticity material model was implemented as user defined material model in the commercial FEM software LS-DYNA. At first, plastic anisotropy will not be considered such that the application of finite plasticity based on a multiplicative split of the total deformation is straightforward. The implementation is based on [13], where the approach has already been extended to incorporate gradient-damage. The flexibility of a user material is necessary especially for our later extension to incorporate the inherent material softening of ductile damage and its physically motivated regularization by gradient-enhancement. In this study, the assumption was made that damage accumulation has no influence on material behavior and is only a failure criterion. An efficient strategy for the implementation of gradient-enhancement in LS-DYNA has been presented recently [14] utilizing the existing thermomechanical coupling.

The isotropic plastic hardening behavior is given by a flow curve presented in [15]. The extrapolated flow curve and the mechanical properties of EN AW-6014 T4 used in this study are shown in Fig. 2. The flow curve was extrapolated according to the Hockett-Sherby approach. The layer compression test is the experimental basis for this extrapolation.

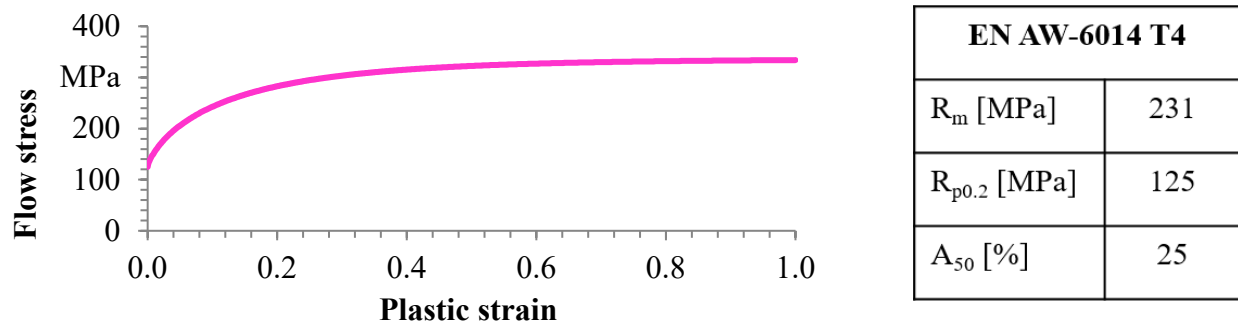


Fig. 2: Mechanical properties of EN AW-6014 T4 [15]

Hosford-Coulomb failure model

The Hosford-Coulomb failure model was proposed in [11]. Therein, the von Mises equivalent stress was replaced by the Hosford equivalent stress in combination with the normal stress acting on the plane of maximum shear. The Hosford-Coulomb model is based on the extensive study on 3D unit cells in [16], thus it has a strong micromechanical foundation. In [11] fracture experiments on three different steels were conducted and used to calibrate the fracture criterion. When compared against the experiments, the simulations showed good agreement. Using and extending previous work [10], the failure prediction is based on the Hosford-Coulomb (HC) failure model [11]. The latter proved most suitable for the failure prediction of the also herein considered aluminum alloy EN-AW 6014. The HC model is the generalization of the Mohr-Coulomb model that was shown to agree well with localization analyses of various stress states [11], which is closely related to the failure prediction. Such stress-state dependent models are well suited to

describe the different damage processes taking place, ranging from void growth to shear banding. The HC failure model predicts the current failure strain $\bar{\epsilon}_f$ as a function of the stress state characterized by the stress triaxiality η and the Lode angle $\bar{\theta}$. For a detailed description of the relations see [11]; [10]. The four parameters of the HC model are taken from [10] for the aluminium alloy EN-AW 6014 T4. Even though at this point, damage-related softening is not activated, a nonlinear damage accumulation law is utilized as proposed in [17]; [18] as

$$dD = n_d \left[\frac{\bar{\epsilon}_p}{\bar{\epsilon}_f(\eta, \theta)} \right]^{n_d-1} \frac{d\bar{\epsilon}_p}{\bar{\epsilon}_f(\eta, \theta)} \quad (1)$$

with the positive damage exponent n_d , here equal to 2. Such an incremental nonlinear approach is regarded as indispensable to predict the damage accumulation under non-proportional loading as present in experiments and distinct for the clinch joining and joint loading.

Results

The clinching process model is compared to the experiment for the connection EN-AW 6014 T4 $t = 2\text{mm}$ in EN-AW 6014 T4 $t = 2\text{mm}$ in order to show the influence of incorrect geometric properties or incorrect plastic deformations that would be calculated based on an incorrect plasticity model. For this purpose, the simulated contour of the clinched joint (blue) is compared with the experimental micro section, as shown in Fig. 3 (left). A good agreement can be observed. Furthermore, the experimental determined force-displacement curve is compared with numerical calculated values. A high agreement between experiment and simulation is evident. The clinched joint mesh calculated in the model is then transferred to the shear load model.

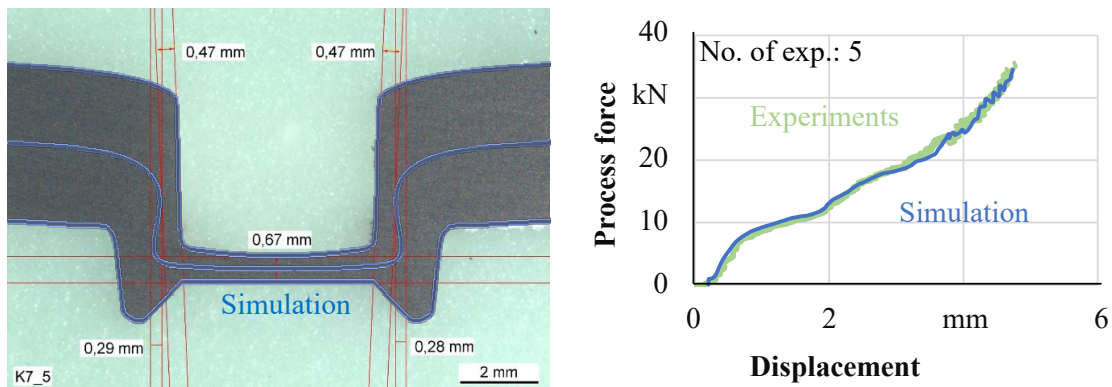


Fig. 3: Model comparison of the clinching process (simulation and experiment)

The element accumulating the highest damage was selected for the localization of the crack location due to the damage accumulation in the shear tensile test. This element was also evaluated in the clinching process. Afterwards, the influence of the joining process induced pre-damage on the shear tensile test was also taken into account (coupled model).

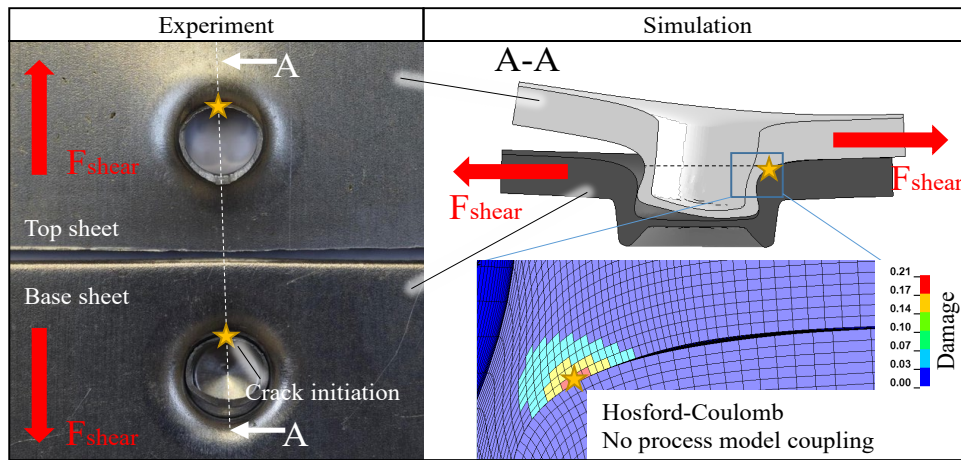


Fig. 4: Localization of the highest damage accumulation in the shear tensile test

The element is located in the top plate in the neck area and is shown in Fig. 4 on the right hand side (marked). The evaluation of the failure location was made at the beginning of the first occurring damage peak. The experimental clinched joint after shear tensile loading is shown on the left, with the fracture location corresponding to the simulated location of the highest damage accumulation. To achieve an understanding of the complex local stress state, the element with the highest final damage was selected and evaluated during the coupled process.

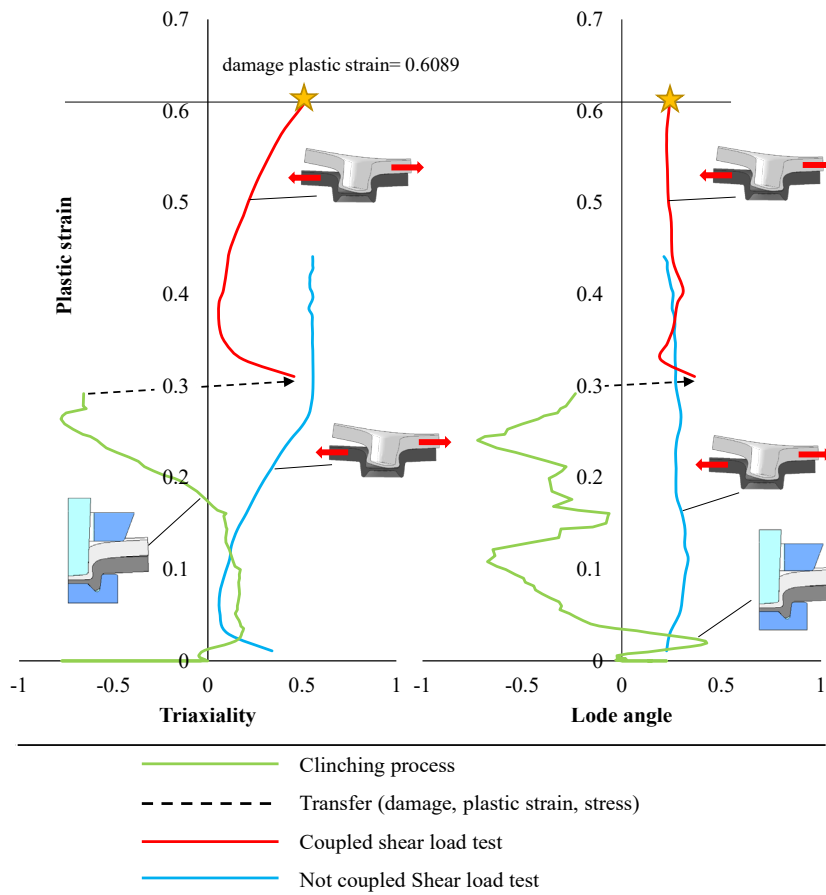


Fig. 5: Simulated stress state during the clinching process and shear tensile test

Fig. 5 shows the plasticity curves of the selected element during the process over the parameters stress triaxiality and the Lode angle, which are used to describe complex stress states.

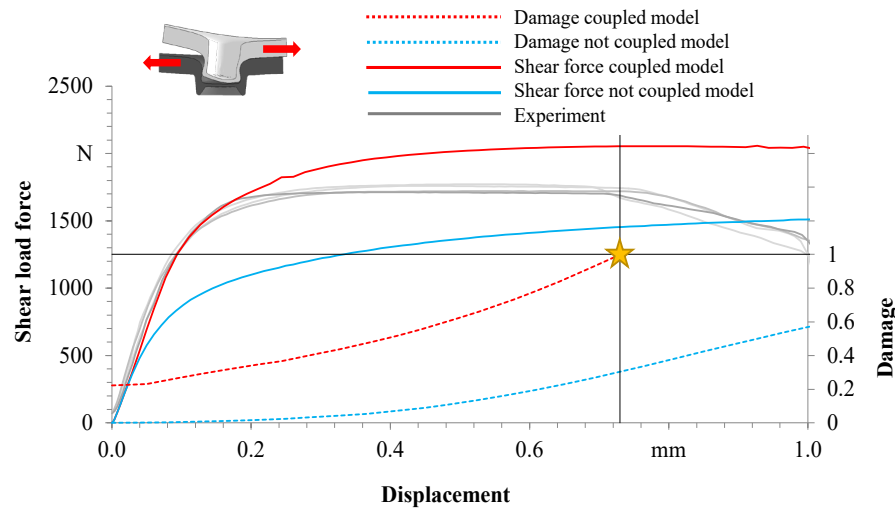


Fig. 6: Force curves during the shear load test and damage accumulation

The blue curve represents the progression of the uncoupled tensile shear test model. Therein, only the geometry (without strains, stresses, damage) was transferred from the clinching process model. The plasticity starts at a value of 0 and increases until the end of the simulation. Since the damage value of 1 is not reached, no failure will occur. The red curve describes the development of local plasticity with coupling to the clinching model, plastic strains, stresses, damage are transferred. Consequently, the red curve starts at an initial plasticity of approx. 0.3. Due to this pre-deformation, the damage accumulates higher, so that the element reaches a damage of 1 at a plasticity of 0.6089 and fails. The qualitative progressions of the uncoupled to the coupled model with regard to stress triaxiality and Lode angle are comparable. Initially, a tension-superimposed stress state is present in the element. In the further course of the test, the punch-sided sheet is pulled over the die-side sheet, which leads to a shear stress in the material, stress triaxiality around 0. The tilting of the specimen and an initial unbuttoning in the joining point (see failure mode in Fig. 4) again leads to a tensile superimposed state, stress triaxiality about 0.5. The green curve shows the plasticity curve of the element selected in the shear test model during the clinching process. The calculated properties (plastic strain, stress, damage) were then transferred to the coupled model (marked by black arrow). Fig. 6 shows the force-displacement curves of the shear tensile test of the coupled (red) and the uncoupled (blue) models. Furthermore, the damage accumulation of the models is also shown, at a value of $D=1$, element deletion occurs and thus a failure of the joint. The uncoupled model underestimates the experimental force-displacement curve, since the strain hardening due to the plastic deformation that occurs in the clinching process is not taken into account. The damage starts at the value 0, since no pre-damage was transferred from the joining process. The damage accumulation in the uncoupled shear tensile test (blue) does not reach a damage value of 1 up to a displacement of 1.0 mm, thus no neck crack is predicted. The coupled model (red) overestimates the force curve of the experiment. Due to the simplified geometry of the FE shear tensile model shown here, a higher specimen stiffness results. Due to the missing total length of the specimen, the bending of the specimen parts characteristic for the specimen shape and the rotating clinch point are omitted, which leads to a simplified joint failure in the regular case. This simplification was adopted for this study, further investigation is required. The deviation of the maximum force can be attributed to the fact that the model does not show any material softening due to the damage. Furthermore, this can be attributed to the use of a quadratic

von Mises yield criterion, which is known to overestimate the yield stress under shear for aluminum materials [19]. In the damage progression of the coupled shear strain model (red), an initial damage can be seen at the beginning. This increases due to the nonlinear Hosford-Coulomb damage accumulation during the shear tensile test until a damage value of 1 is reached. The element fails in the model, which subsequently leads to a neck crack. The simulated predicted failure displacement agrees with the experimental results.

Summary

In this study a modified FE clinching process model was presented, which does not require any remeshing and thus eliminates the influence of remeshing. The Hosford-Coulomb failure model identified in [10] by the modified punch test was implemented in the FE clinching process chain. The damage accumulation in the joining process as well as in the loading process could be determined. The influence of the pre-damage induced in the sheets during the joining process on the shear strength could also be shown. It is important to accumulate the material properties during the whole process chain in order to predict the failure location and time. Furthermore, it was shown that the calibrated Hosford-Coulomb model can predict the failure for the process shown. In further investigations, the material model will be extended to include a non-quadratic yield criterion as well as material softening due to ductile damage using gradient enhancement for appropriate regularization, as presented in [20]. Finally, the damage model is to be implemented in process chain models in order to predict the damage and failure behavior during a pre-operation, the joining process as well as more accurately during the loading phase.

Acknowledgement

This research was funded by the Deutsche Forschungsgemeinschaft, DFG, TRR 285 – project number 418701707 – TRR 285, subproject A01 and A05 is gratefully acknowledged.

References

- [1] G. Meschut, V. Janzen, T. Olfemann, Innovative and Highly Productive Joining Technologies for Multi-Material Lightweight Car Body Structures, *J. of Mater Eng and Perform* 23 (2014) 1515–1523. <https://doi.org/10.1007/s11665-014-0962-3>
- [2] R. Kupfer, D. Köhler, D. Römisch, S. Wituschek, L. Ewenz, J. Kalich, D. Weiß, B. Sadeghian, M. Busch, J. Krüger, M. Neuser, O. Grydin, M. Böhnke, C.-R. Bielak, J. Troschitz, Clinching of Aluminum Materials – Methods for the Continuous Characterization of Process, Microstructure and Properties, *Journal of Advanced Joining Processes* 5 (2022) 100108. <https://doi.org/10.1016/j.jajp.2022.100108>
- [3] C.R. Bielak, M. Böhnke, R. Beck, M. Bobbert, G. Meschut, Numerical analysis of the robustness of clinching process considering the pre-forming of the parts, *Journal of Advanced Joining Processes* 3 (2021) 100038. <https://doi.org/10.1016/j.jajp.2020.100038>
- [4] C.R. Bielak, M. Böhnke, M. Bobbert, G. Meschut, Development of a Numerical 3D Model for Analyzing Clinched Joints in Versatile Process Chains, in: K. Inal, J. Levesque, M. Worswick, C. Butcher (Eds.), *NUMISHEET 2022*, Springer International Publishing, Cham, 2022, pp. 165–172. https://doi.org/10.1007/978-3-031-06212-4_15
- [5] E. Roux, P.-O. Bouchard, Kriging metamodel global optimization of clinching joining processes accounting for ductile damage, *Journal of Materials Processing Technology* 213 (2013) 1038–1047. <https://doi.org/10.1016/j.jmatprotec.2013.01.018>
- [6] P.O. Bouchard, T. Laurent, L. Tollier, Numerical modeling of self-pierce riveting—From riveting process modeling down to structural analysis, *Journal of Materials Processing Technology* 202 (2008) 290–300. <https://doi.org/10.1016/j.jmatprotec.2007.08.077>

- [7] M. Jäckel, T. Grimm, R. Niegsch, W.-G. Drossel, Overview of Current Challenges in Self-Pierce Riveting of Lightweight Materials, in: The 18th International Conference on Experimental Mechanics, MDPI, Basel Switzerland, p. 384.
- [8] M. Otroshi, M. Rossel, G. Meschut, Stress state dependent damage modeling of self-pierce riveting process simulation using GISSMO damage model, *Journal of Advanced Joining Processes* 1 (2020) 100015. <https://doi.org/10.1016/j.jajp.2020.100015>
- [9] A. Rusia, S. Weihe, Development of an end-to-end simulation process chain for prediction of self-piercing riveting joint geometry and strength, *Journal of Manufacturing Processes* 57 (2020) 519–532. <https://doi.org/10.1016/j.jmapro.2020.07.004>
- [10] Böhnke M., Bielak C. R., Friedlein J. Bobbert M. Mergheim J., Meschut G., Steinmann P. (Ed.), A calibration method for damage modeling in clinching process simulations, The 20th International Conference on Sheet Metal, Nuremberg, 2023.
- [11] D. Mohr, S.J. Marcadet, Micromechanically-motivated phenomenological Hosford–Coulomb model for predicting ductile fracture initiation at low stress triaxialities, *International Journal of Solids and Structures* 67-68 (2015) 40–55. <https://doi.org/10.1016/j.ijsolstr.2015.02.024>
- [12] M. Böhnke, M. Rossel, C.R. Bielak, M. Bobbert, G. Meschut, Concept development of a method for identifying friction coefficients for the numerical simulation of clinching processes, *Int J Adv Manuf Technol* 118 (2022) 1627–1639. <https://doi.org/10.1007/s00170-021-07986-4>
- [13] L. Sprave, A. Menzel, A large strain gradient-enhanced ductile damage model: finite element formulation, experiment and parameter identification, *Acta Mech* 231 (2020) 5159–5192. <https://doi.org/10.1007/s00707-020-02786-5>
- [14] J. Friedlein, J. Mergheim, P. Steinmann, Efficient Gradient-Enhancement of Ductile Damage for Implicit Time Integration. Extended abstract of presentation, 16th LS-DYNA Forum 2022, Bamberg, Germany.
- [15] M. Böhnke, F. Kappe, M. Bobbert, G. Meschut, Influence of various procedures for the determination of flow curves on the predictive accuracy of numerical simulations for mechanical joining processes, *Materials Testing* 63 (2021) 493–500. <https://doi.org/10.1515/mt-2020-0082>
- [16] M. Dunand, D. Mohr, Effect of Lode parameter on plastic flow localization after proportional loading at low stress triaxialities, *Journal of the Mechanics and Physics of Solids* 66 (2014) 133–153. <https://doi.org/10.1016/j.jmps.2014.01.008>
- [17] J. Papasidero, V. Doquet, D. Mohr, Ductile fracture of aluminum 2024-T351 under proportional and non-proportional multi-axial loading: Bao–Wierzbicki results revisited, *International Journal of Solids and Structures* 69-70 (2015) 459–474. <https://doi.org/10.1016/j.ijsolstr.2015.05.006>
- [18] M. Nahrman, A. Matzenmiller, Modelling of nonlocal damage and failure in ductile steel sheets under multiaxial loading, *International Journal of Solids and Structures* 232 (2021) 111166. <https://doi.org/10.1016/j.ijsolstr.2021.111166>
- [19] A.M. Habraken, Modelling the plastic anisotropy of metals, *ARCO* 11 (2004) 3–96. <https://doi.org/10.1007/BF02736210>
- [20] J. Friedlein, J. Mergheim, P. Steinmann, A Finite Plasticity Gradient-Damage Model for Sheet Metals during Forming and Clinching, *KEM* 883 (2021) 57–64. <https://doi.org/10.4028/www.scientific.net/KEM.883.57>